Infrared Band Strengths and Other Properties of Three Interstellar Compounds—Amorphous Isocyanic Acid, Formaldehyde, and Formic Acid

Reggie L. Hudson[1] , Yukiko Y. Yarnall[1,2] , and Perry A. Gerakines[1]
[1] Astrochemistry Laboratory, NASA Goddard Space Flight Center, Greenbelt, MD 20771, USA; reggie.hudson@nasa.gov
[2] Center for Space Sciences and Technology, University of Maryland, Baltimore County, Baltimore, MD 21250, USA

Abstract

Infrared (IR) spectral features of interstellar and solar system ices have been attributed to solid organic and inorganic compounds for over 50 yr, but in many cases the laboratory IR data needed to fully quantify such work have never been published, forcing researchers to rely on assumptions about gas- or liquid-phase measurements to interpret data for ices. Here, we report the first mid-IR intensity measurements for isocyanic acid (HNCO) ices that are free of such assumptions, providing new results for use by both observational and laboratory astrochemists. We also report similar new IR data for both formaldehyde (H_2CO) and formic acid (HCOOH), which have been discussed in the astrochemical literature for decades, but again without adequate laboratory data to help quantify observational results. Densities and refractive indices of HNCO, H_2CO, and HCOOH as amorphous ices also are reported. Two applications of the new H_2CO work are presented, the first vapor-pressure measurements of solid H_2CO, along with an enthalpy of sublimation, at 100 to 109 K and a set of IR intensities of H_2CO in $H_2O + H_2CO$ ices. Band strengths, absorption coefficients, and optical constants are calculated for all three compounds. Extensive comparisons are made to older results, which are not recommended for future use.

1. Introduction

For over 50 yr, the study of interstellar and solar system ices has relied on a vigorous program of laboratory work aimed at understanding ice formation, composition, and evolution. Our group's contributions to laboratory studies of extraterrestrial ices began with investigations of radiation-chemical syntheses in ices, followed by studies of both photochemically and thermally induced chemistry, always with an emphasis on infrared (IR) spectroscopy. For a summary with examples, see C. K. Materese et al. (2021).

Over the past decade, we have expanded considerably into the IR quantification of molecules and ions found in interstellar and solar system ices, mostly at temperatures from about 10–150 K. We have found that many of the results from the past that are used to quantify IR astronomical and laboratory spectra of ices are based on techniques and assumptions that unnecessarily introduce errors and uncertainties into the final molecular abundances, sometimes substantial errors. What is just as concerning is that many of those same older results for spectral quantification, particularly IR band strengths, have been carried forward unchecked in the literature to the extent that the original authors' assumptions and qualifications appear to have been forgotten.

Table 1 lists 26 types of compounds, with an example of each, that are either known or suspected to be extraterrestrial. In the far-right column are references to some of our group's work on these same compounds, specifically our IR intensity measurements on each one as a solid. Three blanks are seen, one for the simplest member of the aldehyde, acid, and

isocyanate families. The examples given for those cases, formaldehyde (H_2CO), formic acid (HCOOH), and isocyanic acid (HNCO), have all been studied as solids by laboratory astrochemists, but with results and methods that vary from unverified and problematic to conventional and established, as will be described in this paper.

Isocyanic acid (HNCO) was first identified in the gas phase of the interstellar medium (ISM) in the direction of Sgr B2 by L. E. Snyder & D. Buhl (1972), with cometary HNCO reported later by D. C. Lis et al. (1997). An acid-base reaction between HNCO and NH_3 (ammonia) yields ammonium cyanate, a compound reported in Comet 67/P (K. Altwegg et al. 2020), and the cyanate anion (OCN^-), which is known in the solid phase of the ISM (B. T. Soifer et al. 1979; R. L. Hudson et al. 2001). Reduction of isocyanic acid can lead to formamide, an interstellar molecule. Isocyanic acid also is the prototype isocyanate, two interstellar ones being methyl isocyanate (D. T. Halfen et al. 2015) and ethyl isocyanate (L. F. Rodríguez-Almeida et al. 2021).

Formaldehyde (H_2CO) was the first polyatomic organic molecule identified in the gas phase of the ISM (L. E. Snyder et al. 1969). An interstellar-ice IR feature at $2885 \, cm^{-1}$ ($3.47 \, \mu m$) has been assigned to solid H_2CO, the target object being a protostellar source GL 2136 (W. A. Schutte et al. 1996). However, relatively few robust identifications have been published for H_2CO ices, and those reported appear to be more suggestive than convincing (e.g., Y-L. Yang et al. 2022) due to overlapping IR bands. Formaldehyde has long been known to be a cometary molecule (L. E. Snyder et al. 1989).

The first identification of interstellar gas-phase formic acid, HCOOH, the simplest carboxylic acid, was based on a microwave emission line detected toward Sgr B2 by B. Zuckerman et al. (1971), with a second line reported later by G. Winnewisser & E. Churchwell (1975) from the same source. Both investigations relied on laboratory gas-phase spectroscopic data for the formic acid identification and for abundance

Table 1
Extraterrestrial Ices—IR Intensity Measurements

No.	Family or Type	Compound and Name	Reference
1	alkane	C_2H_6 ethane	[a]
2	alkene	C_2H_4 ethylene	[a]
3	alkyne	C_2H_2 acetylene	[b]
4	diene	CH_2CCH_2 allene	[c]
5	alcohol	CH_3OH methanol	[d]
6	ether	$O(CH_3)_2$ dimethyl ether	[e]
7	aldehyde	H_2CO formaldehyde	
8	ketone	$(CH_3)_2CO$ acetone	[f]
9	acid	HCOOH formic acid	
10	ester	$HC(O)OCH_3$ methyl formate	[g]
11	isocyanate	HNCO isocyanic acid	
12	amine	CH_3NH_2 methylamine	[h]
13	nitrile	CH_3CN acetonitrile	[i]
14	thiol	CH_3SH methanethiol	[j]
15	cyclic, aliphatic	$c\text{-}C_3H_6$ cyclopropane	[k]
16	cyclic, aromatic	C_6H_6 benzene	[l]
17	heterocyclic, aliphatic	$c\text{-}OC_2H_4$ ethylene oxide	[k]
18	heterocyclic, aromatic	C_4H_4N pyridine	[l]
19	diester	$(OCH_3)_2CO$ dimethyl carbonate	[m]
20	carbon oxidized	CO carbon monoxide	[n]
21	carbon reduced	CH_4 methane	[o]
22	nitrogen oxidized	N_2O nitrous oxide	[p]
23	nitrogen reduced	NH_3 ammonia	[q]
24	sulfur oxidized	SO_2 sulfur dioxide	[r]
25	sulfur reduced	H_2S hydrogen sulfide	[r]
26	ammonium salt	NH_4CN ammonium cyanide	[s]

References. (a) R. L. Hudson et al. (2014b); (b) R. L. Hudson et al. (2014a); (c) R. L. Hudson & Y. Y. Yarnall (2022a); (d) R. L. Hudson et al. (2024); (e) R. L. Hudson et al. (2020b); (f) R. L. Hudson et al. (2018); (g) Y. Y. Yarnall & R. L. Hudson (2022c); (h) R. L. Hudson et al. (2022a); (i) M. H. Moore et al. (2010); (j) R. L. Hudson (2016); (k) R. L. Hudson et al. (2023); (l) R. L. Hudson & Y. Y. Yarnall (2022b); (m) R. L. Hudson & F. M. Coleman (2019); (n) Gerakines et al. (2023); (o) P. A. Gerakines & R. L. Hudson (2015a); (p) R. L. Hudson et al. (2017); (q) Hudson et al. (2022b); (r) Y. Y. Yarnall & R. L. Hudson (2022b); (s) P. A. Gerakines et al. (2024).

estimates. W. A. Schutte et al. (1999) suggested that two weak solid-phase features in the IR spectrum of W33A, a young stellar object, might be due to the formate ion, the conjugate base of HCOOH.

Our interest here is in the IR intensities of HNCO, H_2CO, and HCOOH as solids, intensities that are needed to calculate solid-phase molecular abundances from IR spectra. We begin by summarizing some previous work, starting with results from methods that are not widely used and then followed with a description and results from a standard method for measuring IR intensities.

2. Previous Work, ca. 1993–2004

The first measurements of IR intensities of solid HNCO, H_2CO, and HCOOH were done over a roughly 10 yr period, they were restricted to band strengths (A'), and they did not involve the relatively standard methods that had been in place for about 30 yr. For HNCO and H_2CO, A' values were reported for ice mixtures in which one component was used as an internal standard for IR intensity. For example, the paper of F. A. van Broekhuizen et al. (2004) reported a band strength for the strong IR feature of HNCO at $2260\ cm^{-1}$, determined from the loss of HNCO in a reaction with NH_3, the standard adopted,

on warming from about 15 to 122 K. For H_2CO, W. A. Schutte et al. (1993) measured the area of formaldehyde's carbonyl absorbance near $1720\ cm^{-1}$ in an $H_2O + H_2CO$ ice mixture of a specific composition and then, by using the area of that same H_2O ice's libration band as an internal reference, calculated the intensity of the formaldehyde feature in the mixture and also, by extension, in the absence of H_2O.

The approaches just described suffer from multiple problems. Both papers used an internal IR intensity reference from L. B. d'Hendecourt & L. J. Allamandola (1986), but that paper has no details about the number of samples measured for each compound, the thickness of those ices (if more than one), the refractive index used to measure thicknesses, or how the thickness measurements were made. All ice densities were assumed to be $1\ g\ cm^{-3}$, and as explained by P. A. Gerakines et al. (2024) there is an uncertainty of almost 60% in the equation those authors used to determine band areas. (A factor of $\pi/2$ is missing.) For the HNCO study by F. A. van Broekhuizen et al. (2004), it is not clear if the authors' reported HNCO band strength is constant with temperature or is a temperature-averaged value from 15 to 122 K. The H_2CO study of W. A. Schutte et al. (1993) assumed (1) that the reference H_2O band's strength was known, (2) that it was unchanged in the presence of H_2CO, (3) that the H_2O-to-H_2CO ratio in the ice mixture was known, and (4) that the strength of formaldehyde's carbonyl band was the same in the presence and absence of H_2O ice. None of these four assumptions was justified by the authors. Finally, the reference band strength for the libration mode of water ice reported by d'Hendecourt & Allamandola is $2.6 \times 10^{-17}\ cm\ molecule^{-1}$ but W. A. Schutte et al. (1993) gave it as $3.0 \times 10^{-17}\ cm\ molecule^{-1}$ with no explanation for the $\sim$15% increase.

An unconventional approach also was used in an early study of formic acid band strengths by W. A. Schutte et al. (1999). The authors recorded transmission spectra, but instead of measuring band strengths of their HCOOH ices, they analyzed their spectra by using band strengths, again without justification, from *gas-phase* formic acid work (Y. Maréchal 1987). In converting from the original gas-phase units of Y. Maréchal (1987) to those favored by W. A. Schutte et al. (1999), an arithmetic mistake was made by those authors, adding an error of about 5% to the assumed equality of gas- and ice-phase band strengths. Also, the results of Y. Maréchal (1987) were reported with only one significant figure, but an extra figure was added by W. A. Schutte et al. (1999) without explanation.

Even with the problems and concerns described here, these early IR band strengths have been cited frequently in the literature for over 20 yr. For example, from studies in just the past 5 yr, we find H_2CO citations to W. A. Schutte et al. (1993, 1996) by R. G. Urso et al. (2020), E. Congiu et al. (2020), M. Tsuge et al. (2020), W. R. M. Rocha et al. (2021), A. Potapov et al. (2021), P. Herczku et al. (2021), A. L. F. de Barros et al. (2022), and R. Martín-Doménech et al. (2024). Applications cover photo- and radiation chemistry, spectral fitting, and reactions with C and H atoms, and include both interstellar and solar system studies.

These early band-strength measurements for HNCO, H_2CO, and HCOOH (1) did not employ established methods, (2) were not compared to results from them, (3) made multiple assumptions with no justifications provided, and (4) for the two acids they rested on previous work that had problems of its own and that cannot be reproduced. The IR band strengths

from these early studies were, in essence, derived from one-point calibration curves. We do not recommend using the early work, although we recognize it as a pioneering effort.

3. Background to IR Intensity Measurements

For ices of astrochemical relevance, a well-established interferometric method has existed for over 60 yr (J. L. Hollenberg & D. A. Dows 1961) for measuring IR intensities, and it remains the gold standard for such work. In short, IR spectra are recorded for ices of different thicknesses, with each thickness determined by interferometry. Graphs of the absorbance of an IR peak and of the area beneath an IR band are, or should be, linear functions of ice thickness, meaning Beer's Law plots. The slope of the former gives an apparent absorption coefficient, α', and the slope of the latter gives an apparent band strength, A', after division by the ice's number density. The relevant Equations are (1) and (2) below, where h is ice thickness and ρ_N is the sample's number density, in molecules cm^{-3} in our work.

$$\text{Absorbance} \;=\; \frac{\alpha'}{\ln(10)}\,h \qquad (1)$$

$$\int_{\text{band}} (\text{Absorbance})\,d\tilde{\nu} \;=\; \left[\frac{\rho_N A'}{\ln(10)}\right] h. \qquad (2)$$

In each case, the slope must be multiplied by $\ln(10)$ to convert from an absorbance scale (base 10) to an optical depth scale (base e). For determining ice thickness by interferometry, an index of refraction of the ice is needed, which in our work is found by two-laser interferometry (K. E. Tempelmeyer & D. W. Mills 1968). We use a quartz-crystal microbalance in an ultra-high vacuum (UHV) chamber to determine ice densities (C. S. Lu & O. Lewis 1972). R. L. Hudson et al. (2017) has more information, and the papers cited in Table 1 give examples and citations to even earlier work.

A third way in which IR intensities of ices are sometimes expressed is with a sample's complex refractive index, $n(\tilde{\nu}) - ik(\tilde{\nu})$, where $n(\tilde{\nu})$ and $k(\tilde{\nu})$ are optical constants at wavenumber $\tilde{\nu}$. The iterative routine by which we calculate optical constants was described by P. A. Gerakines & R. L. Hudson (2020), and it is still the only free, open-source program for such calculations. Infrared optical constants can be more difficult to calculate than absorption coefficients and band strengths, but they allow for a calculation of an entire spectrum.

The three icy solids considered in this paper are isocyanic acid (HNCO), formaldehyde (H$_2$CO), and formic acid (HCOOH), and infrared spectral intensities have been reported for each compound with the methods just described, although with concerns and difficulties that will be described in the next section. Readers already familiar with the literature on IR intensities of ices might prefer to jump ahead to Section 7 for our new results.

4. Previous IR Intensity Studies Using Interferometric Methods

Infrared band strengths for HNCO ices were first published by M. S. Lowenthal et al. (2002) who used channel (interference) fringes in the baseline of their spectra to determine a refractive index for solid HNCO with which an ice thickness was measured. The authors assumed an ice density of 1 g cm^{-3} for solid HNCO, although ~1.4 g cm^{-3} had been reported earlier (W. C. von Dohlen & G. B. Carpenter 1955). A close reading of

the paper of M. S. Lowenthal et al. (2002) reveals multiple concerns, such as that its Figures 1 and 3 have been exchanged and its Figure 2 appears to show IR spectra of HNCO gas in either a cell with trace H$_2$O or a cell with leaks, judging from the rapidity in which the HNCO contents were destroyed. Spectra were shown after an HNCO ice was formed at 20 K, where it was amorphous, and then after warming to 145 K, after crystallization, but band strengths were reported only for the higher temperature. Another concern, which we return to later, is that the IR spectrum of amorphous HNCO published by M. S. Lowenthal et al. (2002) differs from the one published later by S. Raunier et al. (2003).

The method of J. L. Hollenberg & D. A. Dows (1961) later was used by M. Bouilloud et al. (2015) who examined, among other ices, both H$_2$CO and HCOOH. Refractive indices were needed for ice-thickness measurements and ice densities for obtaining band strengths, but neither quantity was available for either compound, which the authors clearly stated. For amorphous H$_2$CO, a refractive index was "arbitrarily" (those authors' word) chosen and the density of liquid H$_2$CO was adopted for solid H$_2$CO at 25 K. (As an aside, the liquid-phase density was taken from a compilation in a handbook (R. C. Weast & M. J. Astle 1985), but the original source seems to be the density of H$_2$CO at 253 K published by A. Kekulé (1892).) For solid formic acid, data from liquid HCOOH at room temperature were used to analyze the authors' results for solid formic acid at 25 K.

M. Bouilloud et al. (2015) used multiple ices of different thicknesses and Beer's Law plots of band area as a function of ice thickness (or optical depth as a function of column density). M. S. Lowenthal et al. (2002) did not mention similar work. In neither the paper of M. S. Lowenthal et al. (2002) nor that of M. Bouilloud et al. (2015) were integration ranges for IR bands stated, which unnecessarily hinders independent verification of the work reported in each paper.

5. New IR Intensity Studies

As an accurate method for measuring IR intensities in solids has long been known (J. L. Hollenberg & D. A. Dows 1961), it is not necessary to settle for results on HNCO, H$_2$CO, and HCOOH ices that are based on missing reference data, uncertain integration ranges, untested assumptions, or unverified methods when analyzing laboratory spectra or spectra from ground-based or space-based IR observatories, such as the James Webb Space Telescope (e.g., M. K. McClure et al. 2023). Here, we report new laboratory results for solid HNCO, H$_2$CO, and HCOOH, specifically IR intensity measurements that are the first of their type, including absorption coefficients, band strengths, and optical constants. The ice densities and refractive indices needed for accurate results have been measured for the first time and are used, which avoids having to adopt assumed values. Comparisons are made to previous results, although fair and accurate comparisons are difficult due to missing, unreported details. We have recorded a few IR spectra of crystalline ices, but our emphasis is on amorphous solids as they are more directly related to icy mantles of interstellar grains. As part of our work, vapor pressures were measured for both HNCO and H$_2$CO.

We first present results on our two tetratomic molecules, HNCO and H$_2$CO, and then turn to our pentatomic molecule, formic acid (HCOOH). Our interest in H$_2$CO was motivated largely by the molecule's formation in many low-temperature

radiolysis and photolysis experiments and its ability to form more-complex organic molecules (e.g., R. L. Hudson & M. H. Moore 1999). Our work with the acids HNCO and HCOOH was developed in conjunction with our interest in acid–base reactions to make ammonium salts for cometary studies (P. A. Gerakines et al. 2024), but we also have long-standing interests in the conjugate bases of those acids; see our papers on the cyanate (R. L. Hudson et al. 2001) and formate (R. L. Hudson & M. H. Moore 2000) ions in interstellar ices. Additional work is planned with the acids in the future.

6. Laboratory Methods

The methods, procedures, and equipment used for our work have been described in at least a dozen publications from our group. Representative recent papers include those by R. L. Hudson et al. (2022a, 2022b), P. A. Gerakines et al. (2022, 2023), and Y. Y. Yarnall & R. L. Hudson (2022a, 2022b). As recently described for CH_3OH, our IR spectra were measured in a conventional transmission mode with the IR beam perpendicular to the ice sample (R. L. Hudson et al. 2024). Ices were made by gas-phase condensation onto a precooled CsI substrate using an arrangement resembling that in M. H. Moore et al. (2010). Each IR spectrum consisted of 200 accumulations at a resolution of $1 \, cm^{-1}$ from about 7000 to $400 \, cm^{-1}$, with an emphasis on the region from 5000 to $500 \, cm^{-1}$. Refractive indices at 670 nm (n_{670}) and densities (ρ) of ices were measured as described in previous papers (e.g., R. L. Hudson et al. 2017).

The syntheses of HNCO and H_2CO followed procedures used previously in our laboratory as described in H. Cottin et al. (2003) and R. L. Hudson & M. H. Moore (1995), respectively. Isocyanic acid was synthesized by condensing HCl gas (Matheson) onto sodium cyanate, NaOCN (Sigma Aldrich), in a vacuum line. Slow warming initiated a reaction between the two reagents to make HNCO. Residual CO_2 was removed by trapping with an ethanol cryogenic bath at 155 K. Formaldehyde was made by heating polyoxymethylene (Fisher) in an evacuated tube connected to a vacuum line until a pressure of about 10 Torr of H_2CO was reached. Deposition of the H_2CO vapor at 10 K gave an amorphous solid. Ices of formic acid (Acros Organics) were made by condensation of the vapor above liquid HCOOH onto a CsI substrate held at ~10 K. All gas- or vapor-phase condensations to make ices were such as to give an increase in the resulting ice's thickness of a few micrometers per hour. Warming amorphous samples caused crystallization, but the kinetics of the changes were not studied. A few experiments were carried out using triply distilled H_2O with a resistivity greater than 10^7 ohm cm. Both H_2O and HCOOH, each a liquid at room temperature, were degassed with freeze-pump-thaw cycles using liquid nitrogen prior to use.

Vapor pressures for HNCO were measured as described earlier for HCN (P. A. Gerakines et al. 2024). Vapor pressures of H_2CO were determined with the method of R. K. Khanna et al. (1990). The measurement of refractive indices and densities of ices is described by R. L. Hudson et al. (2020a) and Y. Y. Yarnall & R. L. Hudson (2022a). See Yarnall & Hudson (2022b) for the method we used for accurate band-strength measurements in H_2O-rich formaldehyde ices.

Uncertainties in our α' and A' values are about 5% for mid-IR spectra and about 10% for the much weaker features in the near-IR region (Gerakines et al. 2023; R. L. Hudson et al. 2024). See also our allene paper (R. L. Hudson &

Table 2
Refractive Indices and Densities of Ices[a]

Ice	T/K	n_{670}	$\rho/(g \, cm^{-3})$
isocyanic acid, HNCO (amorphous)	19	1.344	1.102
isocyanic acid, HNCO (crystalline)	120	1.517	1.391
formaldehyde, H_2CO (amorphous)	19	1.331	0.933
formaldehyde, H_2CO (crystalline)	90	1.461	1.182
formic acid, HCOOH (amorphous)	15	1.291	0.979

Note.
[a] The HNCO and H_2CO results are new for this work. The HCOOH values are from R. L. Hudson et al. (2020a). Values of n_{670} and ρ are averages of at least three measurements. Uncertainties are about ± 0.005 and $\pm 0.005 \, g \, cm^{-3}$ for n_{670} and ρ, respectively.

Y. Y. Yarnall 2022a) for methods used to estimate these values. See R. L. Hudson et al. (2022c) for comments on uncertainties in vapor pressures, which are estimated to be about 1% over the temperature–pressure range studied, with an uncertainty of $\pm 0.5 \, kJ \, mol^{-1}$ in values of enthalpy of sublimation and an uncertainty of ± 0.5 K in temperature.

7. Results

7.1. Refractive Indices and Ice Densities

Refractive indices of solid HNCO, H_2CO, and HCOOH were needed to determine ice thicknesses by laser interferometry, and such thicknesses, in turn, were needed to obtain IR absorption coefficients, band strengths, and optical constants. Calculations of band strengths also required ice densities. Table 2 shows the results used in this paper, each value being the average of at least three measurements (i.e., three ices).

Measuring these densities and refractive indices required an extra level of effort, but they also improved our work's accuracy. We emphasize that all ice thicknesses in this paper are based on measurements of ices and not the gas-phase pressures, flow rates, or exposure times sometimes used to estimate thicknesses.

7.2. IR Spectra and Vapor Pressures of Solid Isocyanic Acid

Gas-phase deposition of HNCO at 10 K gave an amorphous ice that could be induced to crystallize on slowly warming to about 100 K. Deposition at 120 K gave the crystalline solid directly. Figure 1 shows IR spectra of amorphous and crystalline HNCO made, and the spectra recorded, at 10 and 120 K, respectively. Spectroscopic assignments are given by M. J. Coffey et al. (1999), with illustrations of the vibrations found in S. S. Brown et al. (1997).

Band strengths (A') for six amorphous HNCO ices (thicknesses = 0.12–1.25 μm) were measured for six IR features with the Beer's Law plots for four shown in Figure 2. Absorption coefficients (α') were found as already described. Table 3 lists A' and α' for amorphous HNCO ices along with the integration ranges used. A small absorbance near $3557 \, cm^{-1}$ was judged to be a combination band of the features near 2250 and $1322 \, cm^{-1}$. Its area is not included in our Table 3. Spectra of five crystalline HNCO ices (thicknesses = 0.11–0.55 μm) were recorded and measured, giving the intensity results at the bottom of Table 3.

Vapor pressures for HNCO were measured with a quartz-crystal microbalance in a UHV chamber ($P \sim 10^{-10}$ Torr)
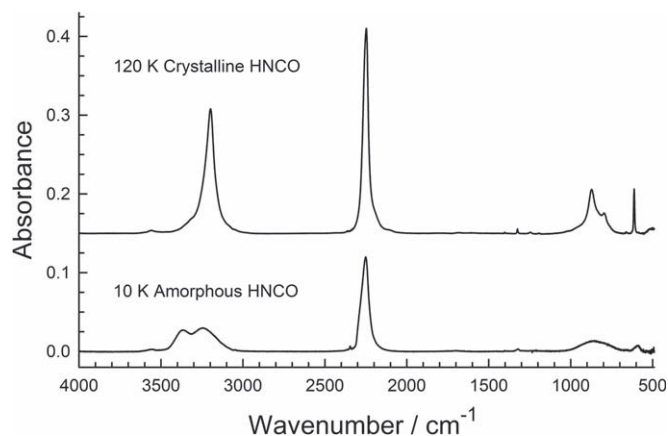
Figure 1. Infrared spectra of amorphous and crystalline HNCO, isocyanic acid, each ice being made and its spectrum recorded at the temperature indicated. Each ice's thickness was about 0.12 μm. The upper spectrum has been offset vertically by 0.15 for clarity.
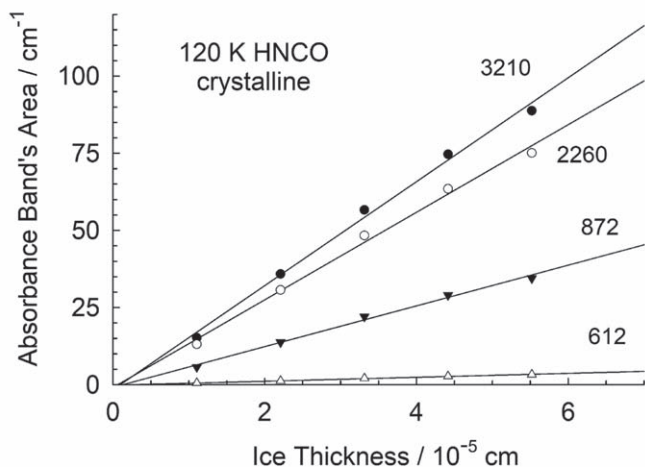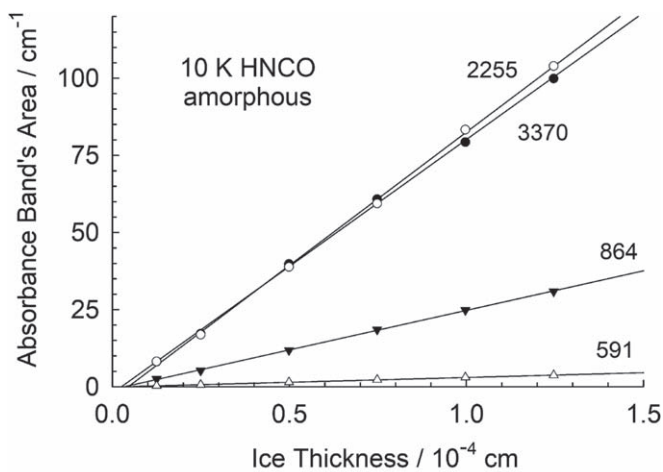
Figure 2. Examples of Beer's Law plots used to determine IR absorption coefficients and band strengths. These are for amorphous and crystalline HNCO, with the ices made and the spectra recorded at 10 and 120 K, respectively.

using the procedure followed by P. A. Gerakines et al. (2024). Triplicate measurements gave average vapor pressures from 119 to 137 K, and a Clapeyron plot (ln P versus $1/T$) gave Equation (3) with a correlation coefficient of 0.999 and with

pressure in Torr and T in Kelvins.

$$\ln(P) = (-5188)\left(\frac{1}{T}\right) + 27.0. \qquad (3)$$

Table 4 lists vapor pressures in intervals of 2 K. Our Clapeyron plot's slope of $(-\Delta H_{subl}/R) = -5188$ K gives the enthalpy of sublimation of crystalline isocyanic acid as $\Delta H_{subl} = 43.1$ kJ mol^{-1}.

7.3. IR Spectra of Solid Formaldehyde

Gas-phase deposition of formaldehyde near 10 K produced an amorphous ice with a spectrum that hardly changed on warming to about 75 K, but that crystallized in just a few minutes at ∼80 K. A faster way to make a crystalline sample was to condense H_2CO at a much higher temperature than 10 K. Infrared spectra of amorphous and crystalline H_2CO ices made at 10 and 90 K, respectively, are shown in Figures 3 and 4, respectively. The spectra in these figures are in good qualitative agreement with earlier work on solid formaldehyde, starting with that of W. G. Schneider & H. J. Bernstein (1956).

Mid-IR band strengths and absorption coefficients are listed in Table 5 for amorphous and crystalline H_2CO, respectively. The table covers the molecule's six fundamental vibrations plus one combination band. A few near-IR bands and peaks were measured at higher wavenumbers (shorter wavelength), and these are given in Table 6. Eight amorphous ices (thicknesses = 0.25–2.01 μm) and five crystalline ices (thicknesses = 0.23–1.15 μm) were used for intensity measurements.

7.4. IR Spectra of Solid Formic Acid

Our work on amorphous HCOOH was done to compare to our H_2CO results and also because of the limited, and somewhat compromised, IR intensities available for solid formic acid. We quickly found, or rather confirmed, that the usual gas-phase condensation method to make HCOOH ices leads to a solid that is dominated by formic acid dimers, $(HCOOH)_2$. See R. C. Millikan & K. S. Pitzer (1957, 1958) for early IR spectroscopic work on the monomeric and dimeric forms of formic acid, and J. Cyriac & T. Pradeep (2005) for a later study. It might not be recognized today by some IR astronomers and laboratory astrochemists, but the IR data used to analyze and quantify formic acid results in ices usually refers to $(HCOOH)_2$ and not to HCOOH. Our goal here was simply to measure IR intensities for solid $(HCOOH)_2$ that improved on those in the literature, while admitting that data for the monomer might be more relevant.

Figure 5 shows a typical spectrum of amorphous formic acid made, and the spectrum recorded, at 10 K. Band strengths and absorption coefficients for four IR features of amorphous HCOOH are given in Table 7. (Seven amorphous ices were used, with thicknesses from 0.52 to 1.56 μm.) Amorphous HCOOH made at ∼10 K could be warmed to initiate crystallization in a few minutes near 125 K, but no quantitative studies of the crystalline solid were undertaken and few spectra were recorded. See J. Cyriac & T. Pradeep (2005) for IR spectra of crystalline formic acid.

7.5. Optical Constants of HNCO, H2CO, and HCOOH

Optical constants were calculated for IR spectra of six amorphous HNCO ices (10 K) and five crystalline ones (120 K), and each set then was averaged to give $n(\tilde{\nu})$ and $k(\tilde{\nu})$. Similarly,

Table 3
Infrared Vibrational Intensities of Amorphous and Crystalline HNCO[a]

Approx. description of vibration	Position $\tilde{\nu}$/cm^{-1}	Position λ/μm	α'/cm^{-1}	Integration range/cm^{-1}	A'/(10^{-18} cm molecule^{-1})
			10 K Amorphous HNCO		
H-N stretch	3368	2.969	7150	3700–2900	122
H-N stretch	3245	3.082	6840	⋯	⋯
NCO asymm-stretch	2250	4.444	27,300	2400–2100	129
NCO symm-stretch	1322	7.564	616	1370–1270	0.956
HNC, NCO bends	857	11.67	3000	1150–677	38.3
NCO in-plane bend	590	16.95	1700	640–540	4.66
			120 K Crystalline HNCO		
H-N stretch	3198	3.127	32,500	3700–2900	199
NCO asymm-stretch	2247	4.450	49,600	2500–1900	168
NCO symm-stretch	1325	7.547	1560	1340–1305	0.662
HNC bend	873	11.45	12,000	1150–677	78.0
NCO out-of-plane bend	796	12.56	4560	⋯	⋯
NCO in-plane bend	612	16.34	11,700	640–580	7.58

Note.
[a] Values of α' and A′ are rounded to three significant figures. See the text for uncertainties. Areas of small features near 3558 and 2346 cm^{-1} were subtracted from integrated regions. Descriptions of vibrations are from S. S. Brown et al. (1997) and M. J. Coffey et al. (1999).
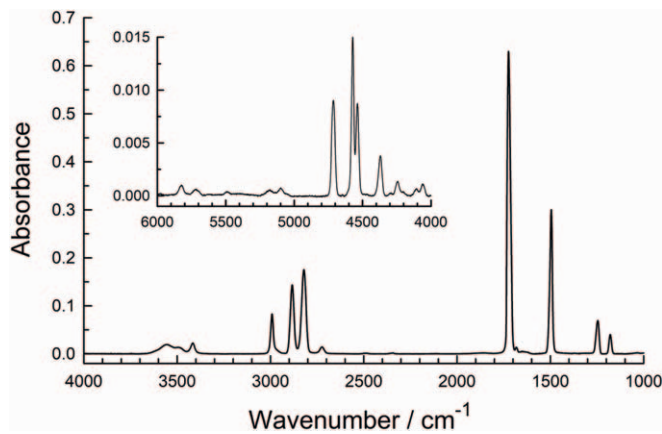
Figure 3. Infrared spectrum of amorphous H$_2$CO, formaldehyde. The ice was made and the spectrum recorded at 10 K. This ice's thickness was about 1.01 μm.
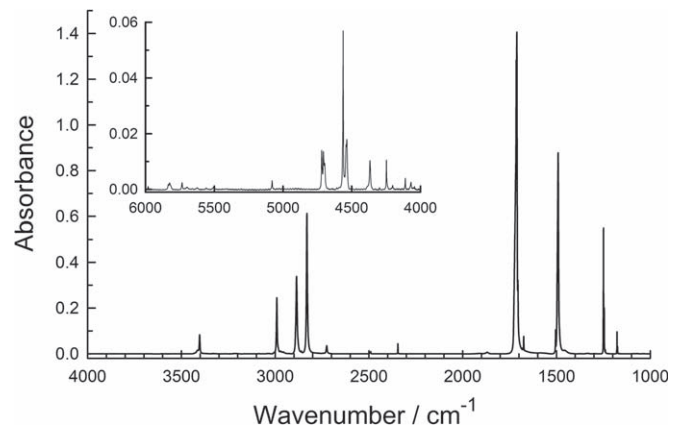
Figure 4. Infrared spectrum of crystalline H$_2$CO, formaldehyde. The ice was made and the spectrum recorded at 90 K. This ice's thickness was about 0.92 μm.

Table 4
Vapor Pressures of Crystalline HNCO[a]

T/K	P/(10^{-8} Torr)
119	5.92
121	12.2
123	24.4
125	48.0
127	92.2
129	174
131	321
133	582
135	1040
137	1820

Note.
[a] Vapor pressures rounded to three significant figures. Values at other temperatures can be found by using Equation (3). Vapor-pressure uncertainties are about 1%. See the text.

$n(\tilde{\nu})$ and $k(\tilde{\nu})$ were calculated for eight amorphous H$_2$CO ices and five crystalline ones at 10 and 90 K, respectively, and averaged. Finally, optical constants were calculated for seven amorphous HCOOH ices at 10 K and averaged. These were the same ices used for the calculations of α' and A' already described.

As an example of our optical-constants results, Figures 6 and 7 show $n(\tilde{\nu})$ and $k(\tilde{\nu})$ for mid- and near-IR regions for amorphous H$_2$CO. All constants are posted to The Cosmic Ice Laboratory, and copies of the infrared spectra and optical constants have also been deposited to Zenodo.[3]

7.6. Application #1—Vapor Pressures of H$_2$CO

The lack of vapor pressures for H$_2$CO ices was noted by N. Fray & B. Schmitt (2009) in their bibliographic review of the sublimation of ices. C. M. Lisse et al. (2021) also mentioned a lack of thermodynamic data for H$_2$CO in their modeling work on the ices of Pluto and Arrokoth. Having formaldehyde in hand, it thus seemed reasonable to investigate its sublimation and resulting vapor pressures. However, we decided not to use our preferred method for vapor-pressure determinations, a quartz-crystal microbalance in a UHV chamber, for fear that the

---

Table 5
Infrared Vibrational Intensities of Amorphous and Crystalline H_2CO[a]

| Approx. description of vibration[b] | 10 K Amorphous H_2CO | | | | |
	Position $\tilde{\nu}$/cm^{-1}	Position λ/μm	α'/cm^{-1}	Integration range/cm^{-1}	A'/(10^{-18} cm molecule^{-1})
Combination band	2991	3.34	1850	3032–2925	2.00
CH_2 asymm-stretch[c]	2884	3.47	3100	2921–2778[c]	3.98
CH_2 symm-stretch[c]	2821	3.54	3880	2921–2778[c]	6.01
C=O stretch	1724	5.80	14,400	1747–1590	16.3
CH_2 scissoring	1495	6.68	6520	1529–1418	5.92
CH_2 rocking	1246	8.02	1480	1277–1200	1.57
CH_2 wagging	1179	8.48	867	1200–1144	0.756
	90 K Crystalline H_2CO				
Combination band	2991	3.34	6160	3015–2976	1.47
CH_2 asymm-stretch	2886	3.46	8620	2911–2856	3.27
CH_2 symm-stretch	2831	3.53	14,600	2856–2795	4.41
C=O stretch	1711	5.84	31,800	1750–1681	16.9
CH_2 scissoring	1491	6.70	20,100	1527–1428	7.92
CH_2 rocking	1249	8.00	13,900	1260–1228	1.50
CH_2 wagging	1177	8.49	2420	1183–1167	0.176

Notes.
[a] The values of α' and A$'$ are rounded to three significant figures. See the text for uncertainties.
[b] Descriptions from K. B. Harvey and J. F. Ogilvie (1962) and H Khoshkhoo & E. R. Nixon (1973).
[c] The two CH_2 stretching bands overlapped slightly, and so curve fitting (with Gaussian functions) was used to determine the area of each band.

Table 6
Intensities of Selected Near-IR Absorptions of H_2CO Ice[a]

Ice and temperature	Position $\tilde{\nu}$/cm^{-1}	Position λ/μm	α'/cm^{-1}	Integration range/cm^{-1}	A'/(10^{-18} cm molecule^{-1})
amorphous, 10 K	5825	1.71	18	5862–5772	0.0323
amorphous, 10 K	4714	2.12	197	4750–4662	0.327
amorphous, 10 K	4571	2.19	323	4622–4495	0.614
crystalline, 90 K	5981	1.67	26	6015–5946	0.0105
crystalline, 90 K	5825	1.71	57	5858–5793	0.0491
crystalline, 90 K	5734	1.74	60	5761–5679	0.0348
crystalline, 90 K	4563	2.19	1490	4589–4511	0.609

Note.
[a] The values of α' and A$'$ are rounded to three significant figures. See the text for uncertainties.
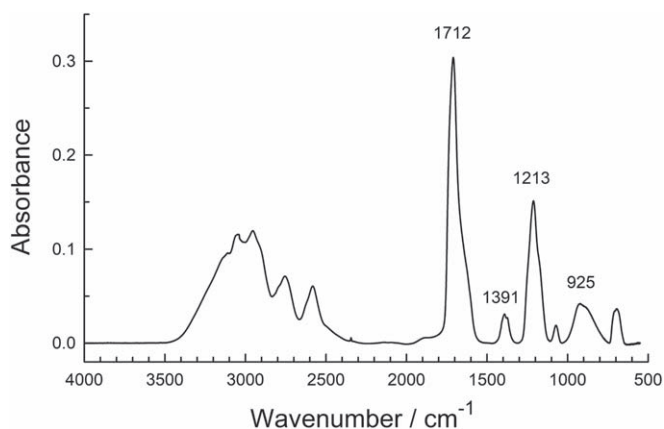
Figure 5. Infrared spectrum of amorphous formic acid. The ice was made and the spectrum recorded at 10 K. This ice's thickness was about 0.52 μm.

microbalance's surface would be severely damaged were our formaldehyde to polymerize on warming.

The method we used to measure vapor pressures of solid H_2CO was described by R. K. Khanna et al. (1990) and involves measuring IR spectra of an ice during its sublimation.

The technique resembles the Knudsen method connecting a flux of subliming molecules to a vapor pressure of the material being studied. For the present work, we deposited H_2CO at 90 K and warmed it to initiate sublimation. By recording the decrease in band areas of IR features of known band strength, at 1711, 1491, and 1249 cm^{-1}, the flux of molecules subliming was calculated. From there the vapor pressures in Table 8 were found. A fit to a Clapeyron plot (ln P versus $1/T$) gave Equation (4) with a correlation coefficient of 0.999 and with pressure in Torr and T in Kelvins.

$$\ln(P) = (-4188)\left(\frac{1}{T}\right) + 25.3. \quad (4)$$

The Clapeyron plot's slope of $(-\Delta H_{subl}/R) = -4188$ K gives the enthalpy of sublimation of crystalline formaldehyde as $\Delta H_{subl} = 34.8$ kJ mol^{-1}.

7.7. Application #2—IR Spectral Intensities of $H_2O + H_2CO$ Ices

The high abundance of solid H_2O in interstellar ices suggests that it might alter IR band strengths of some compounds. To

Table 7
Intensities of Selected Mid-IR Absorptions of Amorphous Formic Acid[a] at 10 K[b]

Approximate description [c]	Position $\tilde{\nu}$/cm^{-1}	Position λ/μm	α'/cm^{-1}	Integration range/cm^{-1}	A'/(10^{-18} cm molecule^{-1})
C=O stretch	1712	5.84	14900	1800–1500	96.0
HCO bending	1391	7.19	1410	1460–1311	6.44
C–O stretch	1213	8.24	6750	1308–1108	42.3
COH bending	925	10.8	1720	1033–740	20.3

Notes.
[a] The ice is composed largely of formic acid dimers, $(HCOOH)_2$.
[b] Values of α' and A' are rounded to three significant figures. See the text for uncertainties.
[c] Descriptions from R. C. Millikan and K. S. Pitzer (1957, 1958) and Y. Maréchal (1987).
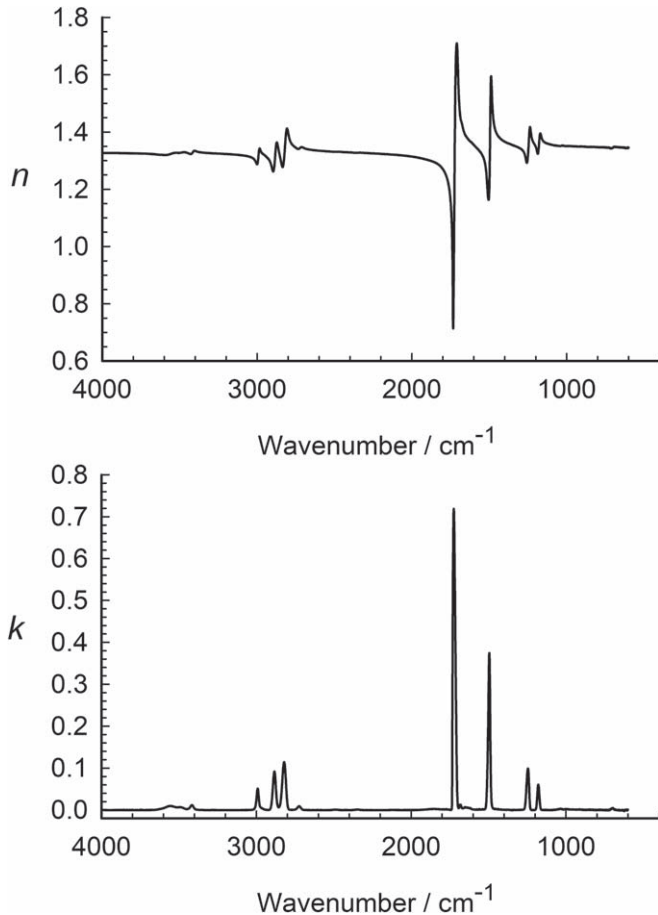
Figure 6. Mid-IR optical constants of amorphous H_2CO, formaldehyde. Values of n and k were calculated from the IR spectra of eight ices and then averaged to give the results shown here. Each ice was made and its spectrum was recorded at 10 K. The ices used to calculate these optical constants varied in thickness from about 0.25 to 2.01 μm.

Figure 7. Near-IR optical constants of amorphous H_2CO, formaldehyde. Values of n and k were calculated from the IR spectra of eight ices and then averaged to give the results shown here. Each ice was made and its spectrum was recorded at 10 K. The ices used to calculate these optical constants varied in thickness from about 0.25–2.01 μm.

test this possibility for formaldehyde, we prepared H_2O + H_2CO ice mixtures with H_2O as the dominant component and recorded their IR spectra. Our procedure, described by Yarnall & Hudson (2022b), avoids all use of gas-phase band strengths and the rather common assumption that a multicomponent ice has the same composition as the multicomponent gas-phase mixture from which it was prepared.

For our study, we prepared H_2O + H_2CO ices with ratios of 8.5:1 and 28:1, condensing the vapor of each compound through its own deposition line. Plots of H_2CO band areas as a function of H_2CO column density (or, equivalently, ice

Table 8
Vapor Pressures of Crystalline H_2CO[a]

T/K	P/(10^{-8} Torr)
100	6.17
105	45.3
107	95.4
109	196

Note.
[a] Vapor pressures rounded to three significant figures. Values at other temperatures can be found by using Equation (4). Vapor-pressure uncertainties are about 1%. See the text.
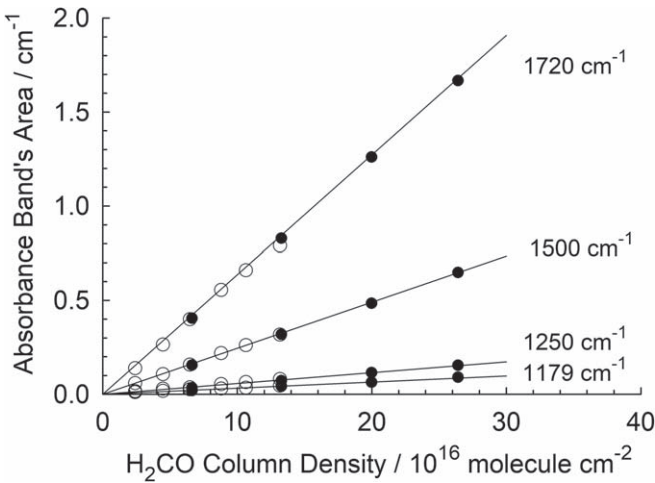
Figure 8. Beer's Law plots used to determine IR band strengths for H_2CO in $H_2O + H_2CO$ ices with the ices made and the spectra recorded at 10 K. Open (white) circles are for six $H_2O + H_2CO$ (28:1) ices and closed (black, filled) circles are for four $H_2O + H_2CO$ (8.5:1) ices.

thickness) were linear with slopes that again gave band strengths. Four examples are shown in Figure 8, with final numerical results in Table 9.

8. Discussion

8.1. Refractive Indices and Ice Densities

There are no published values of amorphous isocyanic acid's density (ρ) and refractive index (n) with which to compare our results. However, to the extent that amorphous solids are comparable to frozen liquids, our density of amorphous HNCO, $\rho(19\,K) = 1.102\,g\,cm^{-3}$, compares favorably with $1.14\,g\,cm^{-3}$ for the liquid at $20°C$ (R. C. Weast & M. J. Astle 1980). Our density for crystalline HNCO is ρ $(120\,K) = 1.391\,g\,cm^{-3}$ and is similar to the $\rho(148\,K) = 1.41\,g\,cm^{-3}$ in a diffraction study of W. C. von Dohlen & G. B. Carpenter (1955).

There also are no published values of amorphous formaldehyde's density and refractive index for comparison to our results. Again to the degree that amorphous solids are comparable to frozen liquids, our density of amorphous H_2CO, $\rho(19\,K) = 0.933\,g\,cm^{-3}$, is about as expected from $\rho(193\,K) = 0.9172\,g\,cm^{-3}$ (A. Kekulé 1892) for the liquid. A better comparison is between that of our $\rho(90\,K) = 1.182\,g\,cm^{-3}$ for crystalline formaldehyde and $\rho(148\,K) = 1.167\,g\,cm^{-3}$ from a diffraction study of the solid (T. S. Thakur et al. 2011).

The agreement between our ρ and n for amorphous formic acid and the room-temperature values of $1.220\,g\,cm^{-3}$ and 1.3714 (R. C. Weast & M. J. Astle 1980) is not as good, perhaps reflecting complications from the monomer-dimer issue already mentioned.

Another type of comparison comes from values of molar refraction, R_m, defined in Equation (5).

$$R_m = \left(\frac{M}{\rho}\right)\left(\frac{n^2 - 1}{n^2 + 2}\right). \qquad (5)$$

Using formaldehyde's molar mass, $M = 32.03\,g\,mole^{-1}$, and the data in Table 2, we find $R_m = 6.58\,cm^3\,mole^{-1}$ for the amorphous solid. Molar refractions are approximately additive by bond types and functional groups (e.g., K. G. Denbigh 1940), so for comparison we chose the next three larger aldehydes,

acetaldehyde ($HC(O)CH_3$), propionaldehyde ($HC(O)CH_2CH_3$), and butyraldehyde ($HC(O)CH_2CH_2CH_3$), with each having one more CH_2 group than the previous compound. The values of n, ρ, and R_m for these aldehydes were reported in R. L. Hudson et al. (2020a). Figure 9 shows the R_m values for all four aldehydes, with the least-squares line leading down to the left to the $6.58\,cm^3\,mole^{-1}$ we found for formaldehyde. The fit is reasonable, with a correlation coefficient of 0.9961. Figure 10 shows a similar comparison of R_m for HCOOH to values for $HC(O)OCH_3$, $CH_3C(O)OCH_3$, and $CH_3CH_2C(O)OCH_3$, each compound having one more CH_2 group than the one before it, and a slightly higher R_m value. Again, the fit for the four points, reaching down to the $R_m = 8.55\,cm^3\,mole^{-1}$ on the lower left for amorphous formic acid, seems reasonable, with a correlation coefficient of 0.9996.

8.2. A Comment on Comparisons

As stated in Section 2, we do not recommend using band strengths from Schutte and colleagues for H_2CO (W. A. Schutte et al. 1993), HCOOH (W. A. Schutte et al. 1999), and HNCO (F. A. van Broekhuizen et al. 2004). The results in those three papers are problematic due to untested assumptions, unverified methods, and errors in calculations. For these reasons, meaningful quantitative comparisons to the present work are impossible. In cases where those older results might resemble the present ones, it would be impossible to know if such apparent agreement was from anything more than serendipity or offsetting errors. Conversely, unambiguous conclusions also could not be drawn in cases of disagreement with the present study.

In the following sections we compare our quantitative results to those of M. S. Lowenthal et al. (2002) for HNCO and to the work of M. Bouilloud et al. (2015) on H_2CO and HCOOH.

8.3. IR Spectra and Intensities—HNCO

Some differences between the amorphous-HNCO spectra of M. S. Lowenthal et al. (2002) and S. Raunier et al. (2003) have already been mentioned. Figure 11 compares one of our amorphous-HNCO spectra with one scanned from each of those papers. Rather striking differences are seen between the spectrum of M. S. Lowenthal et al. (2002) at the top and the other two spectra in terms of the widths and relative heights of the bands near 3300, 2250, and 1000–800 cm^{-1}. The two broad features near 3300 cm^{-1} in our spectrum are missing from the upper trace, and the small splitting there of $\sim25\,cm^{-1}$ contrasts with a separation of $\sim123\,cm^{-1}$ in our spectrum. In M. S. Lowenthal et al. (2002), the height of the strong IR peak near 3300 cm^{-1} is slightly greater than that of the one at 2250 cm^{-1}, but the heights are very different and in the opposite direction in the spectra from our lab and from S. Raunier et al. (2003), even though the latter spectrum was obtained in a reflection mode. The shape and position of the absorbance at 1000 to 800 cm^{-1} from M. S. Lowenthal et al. (2002) also disagrees with our result.

Our interpretation of these differences is that the HNCO ice of M. S. Lowenthal et al. (2002), although made at 20 K, was a mixture of amorphous and crystalline components, which will have stronger IR bands than will a purely amorphous sample. Partial crystallization might have been caused by the deposition temperature being higher than the stated 20 K or by a rapid rate of HNCO condensation and the accompanying energy release, but no deposition rate was given by M. S. Lowenthal et al. (2002). In short, no quantitative
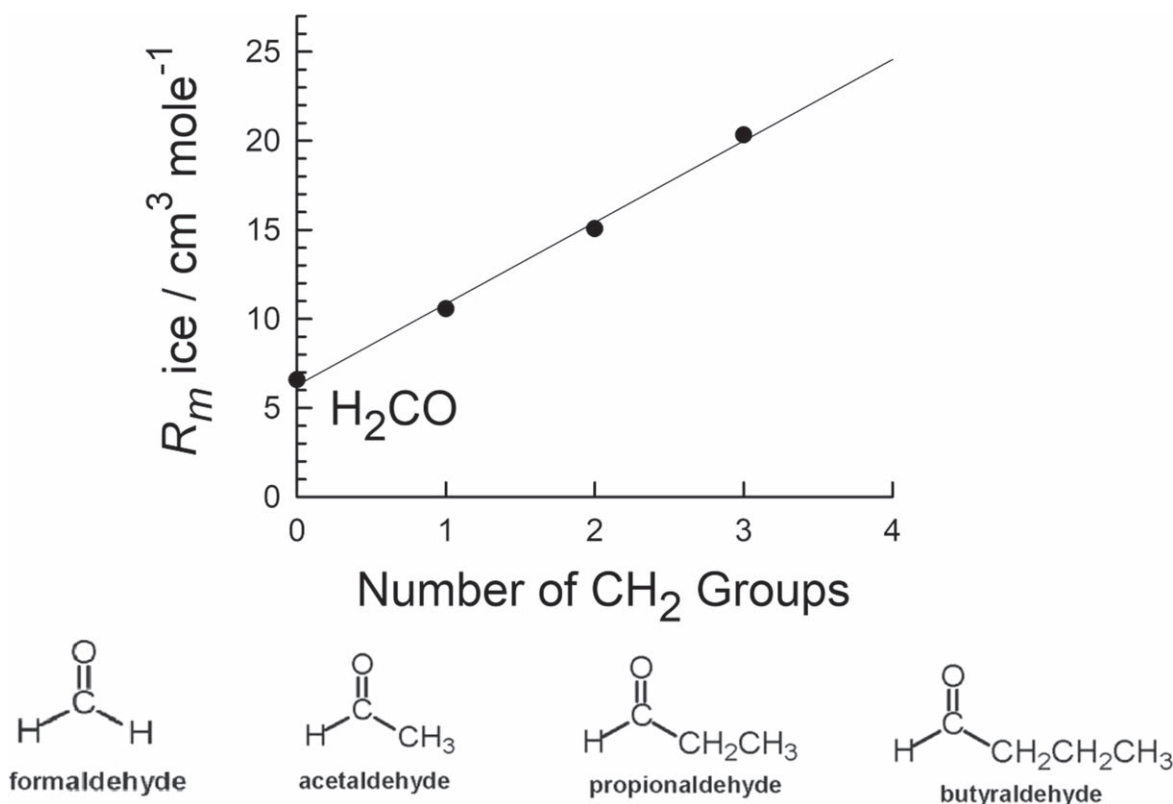
Figure 9. Molar refractions of four amorphous aldehyde ices as a function of the number of methylene (-CH$_2$-) groups of the molecule. From the lower left to the upper right in the graph, the points are for formaldehyde, acetaldehyde, propionaldehyde, and butyraldehyde (R. L. Hudson et al. 2020a).

Table 9
Band Strengths of Amorphous H$_2$CO-containing Ices at 10 K[a]

Integration Range/cm^{-1}	Peak Position		$A'/(10^{-18}$ cm molecule$^{-1})$		
	$\tilde{\nu}$/cm^{-1}	λ/µm	H$_2$O:H$_2$CO (28:1)	H$_2$O:H$_2$CO (8.5:1)	H$_2$CO[b]
1745–1700	1720	5.81	14.2	14.7	16.3
1521−1476	1500	6.67	5.59	5.73	5.92
1270−1228	1250	8.00	1.37	1.43	1.57
1200−1159	1179	8.48	0.694	0.821	0.756

Notes.
[a] The preparation of H$_2$O-rich ices used n_{670}(H$_2$O) = 1.234 and ρ(H$_2$O) = 0.719 g cm^{-3} (Y. Y. Yarnall & R. L. Hudson 2022b) to determine the H$_2$O:H$_2$CO ratio.
[b] The integration ranges and peak positions for neat H$_2$CO in the final column differ slightly from those in the first three columns. They can be found in Table 5.

comparisons are possible between our amorphous-HNCO spectra and that of M. S. Lowenthal et al. (2002) because those authors' ice was at least partially crystalline.

It initially was thought that an accurate quantitative comparison could be made between our results and the crystalline HNCO band strengths of M. S. Lowenthal et al. (2002). This did not prove to be the case. The crystalline ice of M. S. Lowenthal et al. (2002) was made by warming from 20 K, and so in Figure 12 we show their published spectrum alongside one of ours, the ice being made at 10 K and warmed to 110 K. It again is quickly seen that the differences in relative band areas are substantial. The breadth of the bands near 3300 and 2250 cm^{-1} is much larger in (a) than in (b), and the relative area of the broad band from about 1000 to 800 cm^{-1} is far greater in (a) than in (b). Our interpretation this time is that the crystalline ice of M. S. Lowenthal et al. (2002) was sufficiently thick to reach a saturation level for the features near 3300 and

2250 cm^{-1}, giving rise to the large widths and flat peaks seen. Any analysis and comparison of IR band intensities of such drastically different spectra as (a) and (b) in Figure 12 would be less of a quantitative analysis than wishful thinking.

We should point out here that our spectrum (b) in Figure 12, for an ice that had been crystallized by warming, differs slightly from that of crystalline HNCO in Figure 1, for an ice made by deposition at 120 K. Specifically, from about 1000–700 cm^{-1} two sharp peaks are seen in Figure 1 (upper trace), but at least three small features can be seen in Figure 12 (lower trace). We suggest that the reason for these differences is that only one crystalline phase of HNCO is present in Figure 1, but *two crystalline phases of HNCO* are present in Figure 12, in both our spectra and in that of M. S. Lowenthal et al. (2002). This is not an entirely new suggestion as two crystalline phases of HNCO were reported by W. C. von Dohlen & G. B. Carpenter (1955) in a diffraction study. The HNCO crystal structure of
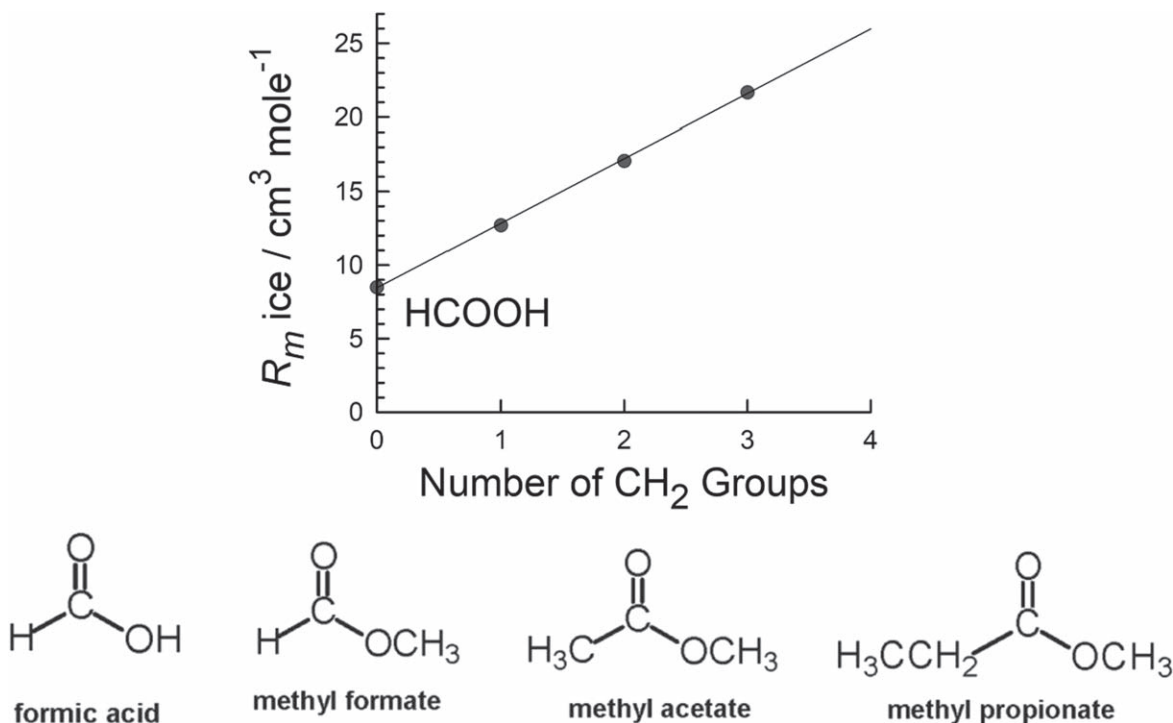
Figure 10. Molar refractions of four amorphous ices as a function of the number of methylene (-CH$_2$-) groups of the molecule. From the lower left to the upper right in the graph, the points are for formic acid, methyl formate, methyl acetate, and methyl propionate. Values of R_m are from R. L. Hudson et al. (2020a).
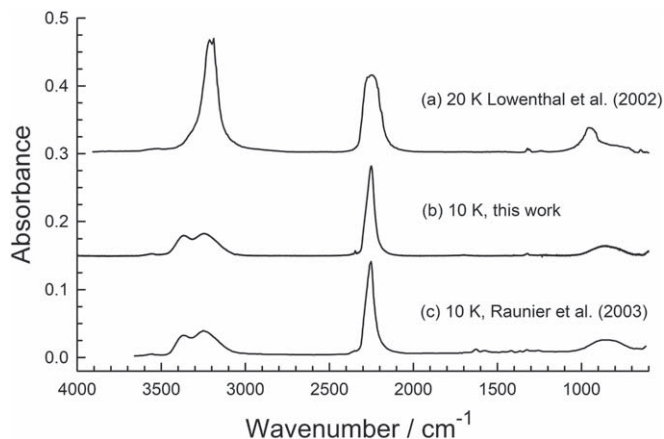
Figure 11. Three infrared spectra of solid isocyanic acid, HNCO, scaled to the same height. (a) Transmission mode, scanned from M. S. Lowenthal et al. (2002), (b) transmission mode, this work, (c) reflection mode, scanned from S. Raunier et al. (2003). Each ice was made and the spectrum recorded at the temperature indicated.

J. Evers et al. (2018) had a higher density than what we measured, so we take our ice as being of the high-temperature polymorph reported by W. C. von Dohlen & G. B. Carpenter (1955). Clearly, more work is needed to unravel the IR spectra of the two crystalline forms of HNCO.

A comparison also can be made between the IR band strength of isocyanic acid's asymmetric stretching vibration and band strengths of related molecules. The HNCO molecule, with three non-H atoms and 16 valence electrons, is isoelectronic with three other molecules that we have studied, CO_2, N_2O, and allene. Isocyanic acid's NCO bond angle is slightly less than the 180° about the central atom of each of the other three molecules (J. Evers et al. 2018), but all four are examples of cumulated bonding, meaning three contiguous

atoms with double bonds about the central atom. In Table 10 we compare the IR band strengths of the intense asymmetric stretching mode of these same four molecules, and it is seen that HNCO is the strongest absorber for both forms of these solids. The $A' = 1.29 \times 10^{-16}$ cm molecule^{-1} of HNCO also is essentially the same as $A' = 1.20 \times 10^{-16}$ cm molecule^{-1} for OCS, carbonyl sulfide, another cumulated molecule we have studied (Yarnall & Hudson 2022b).

8.4. IR Spectra and Intensities—H$_2$CO

As already stated, our formaldehyde spectra in Figures 2 and 3 are in qualitative agreement with those in the literature. However, this applies only to the mid-IR region from about 4000 to 400 cm^{-1} as we have not found comparison spectra of solid H$_2$CO at higher wavenumbers (i.e., shorter wavelengths). Table 11 shows that the mid-IR band strengths for amorphous H$_2$CO published by M. Bouilloud et al. (2015) are in reasonable agreement with our own. More precise comparison is difficult as those authors did not report results with the same details provided here. Moreover, their amorphous-H$_2$CO spectrum differs slightly from ours around 3500 and 1700 cm^{-1}, but not that of W. A. Schutte et al. (1996), so closer agreement in band strengths might not be possible.

In comparing our formaldehyde results to those of M. Bouilloud et al. (2015), we found a contradiction involving those authors' Figure 11, its caption, and the tabulated band strengths for H$_2$CO. Our measurements of H$_2$CO spectra from eight amorphous ices at 10 K gave 21.1 cm^{-1} as the ratio of band area to peak height near 1724 cm^{-1}. That same peak's height in the spectrum of M. Bouilloud et al. (2015) is about 0.82, so that the integrated optical depth of that band is $21.1 \times 0.82 = 17.3$ cm^{-1}. However, that same figure's caption gives the H$_2$CO column density as $N = 2.4 \times 10^{18}$ molecules cm^{-2}, which can be combined with that paper's band strength

Table 10
IR Band Strengths ($A'/(10^{-18}$ cm molecule^{-1})) of Four Compounds[a]

Form	HN=C=O Isocyanic Acid	O=C=O Carbon Dioxide	N=N=O Nitrous Oxide	H$_2$C=C=CH$_2$ Allene (Propadiene)
amorphous	129	118	58.9	8.74
crystalline	168	76.4	51.0	8.38

Note.
[a] Each band strength is for the asymmetric vibration about the molecule's central atom, but C in the case of HNCO. Note that HNCO is quasi-linear as the NCO angle is slightly smaller than 180°. Values for HNCO are from this work, those for CO$_2$ are from P. A. Gerakines & R. L. Hudson (2015b) and H. Yamada & W. B. Person (1964), those for N$_2$O are from R. L. Hudson et al. (2017), and those from allene are from R. L. Hudson & Y. Y. Yarnall (2022a).

Table 11
Band Strengths ($A'/(10^{-18}$ cm molecule^{-1})) of Amorphous H$_2$CO

Approximate Band Position/cm^{-1}	M. Bouilloud et al. (2015)	This Work	% Difference
2882	4.7	3.98	−15
1724	16	16.3	2
1500	5.1	5.92	16
1244	1.5	1.57	5
1177	0.72	0.756	5
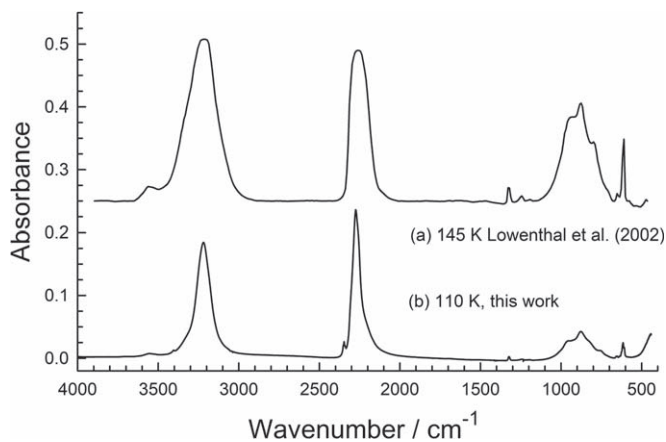
Figure 12. Two infrared spectra of solid isocyanic acid, HNCO, scaled to the same height, both recorded in transmission, (a) scanned from M. S. Lowenthal et al. (2002) and (b) from an ice in this work. See the text for details.

of $A' = 1.6 \times 10^{-17}$ cm molecule^{-1} to give an integrated optical depth according to Equation (6) below.

$$\int_{\mathrm{band}} (\tau)\, d\tilde{\nu} = N\, A' = (2.4 \times 10^{18})(1.6 \times 10^{-17}) = 38.4 \text{ cm}^{-1}.$$
(6)

This result of 38.4 cm^{-1} is about 120% larger than the expected 17.3 cm^{-1}. The source of this difference is unknown, but it is does not alter conclusions of the present work or the comparisons in our Table 11.

8.5. IR Spectra and Intensities—HCOOH

Comments about the earlier band-strength measurements of H$_2$CO ices also apply to solid HCOOH, such as the number of ices examined and integration limits. The most serious concern from an astrochemical perspective is that the previous work and that presented here are for amorphous formic acid ices consisting of the dimer, (HCOOH)$_2$. To our knowledge, solid-phase spectra of monomeric formic acid have not been published, aside from matrix-isolation studies (e.g., M. Halupka & W. Sander 1998).

Table 12
Band Strengths of Amorphous (HCOOH)$_2$, $A'/(10^{-18}$ cm molecule^{-1})

Position/cm^{-1}	M. Bouilloud et al. (2015)	This Work	% Difference
1708	54	96.0	78
1384	3.7	6.44	74
1216	29	42.3	46
929	64	20.3	−68

Table 12 compares the published band strengths of amorphous formic acid of M. Bouilloud et al. (2015) to our new measurements. The agreement with the present work is not especially good. Perhaps the most striking difference is that the intensity of the formic acid band at 929 cm^{-1} is listed as larger than that of the strong 1708 cm^{-1} carbonyl feature, which our Figure 5 shows is incorrect.

Figure 13 shows four different comparisons. In graph (a), a strong correlation of relative band strengths is seen between our values in Table 7 and the gas-phase band strengths of Y. Maréchal (1987). Graph (b) shows a much weaker correlation for the values of M. Bouilloud et al. (2015). Graph (c) compares our band strengths to those published by M. Bouilloud et al. (2015). For graph (d), we digitized and integrated the spectrum published by Bouilloud et al. estimating their ice's thickness with our absorption coefficient for the C=O band and using our density to calculate band strengths. The resulting agreement is quite good. Given the high correlation and the slope near 1, the differences seen in Table 12 are surprising, and for which we offer no explanation.

As already mentioned, our IR spectra for amorphous formic acid are for dimers of the molecule, not monomers. To estimate band strengths of the monomer, it might seem intuitive to simply divide our A' values by 2, but we have no firm justification for this practice. That some type of adjustment is needed is suggested by Table 13, which compares IR intensities of carbonyl features we have measured in three other amorphous ices. The value for formic acid, in the last line, seems much too large in comparison. The only other molecule in Table 13 with the HC(=O)O framework of formic acid is methyl formate. Division of A' for dimeric formic acid's carbonyl band by 2 gives
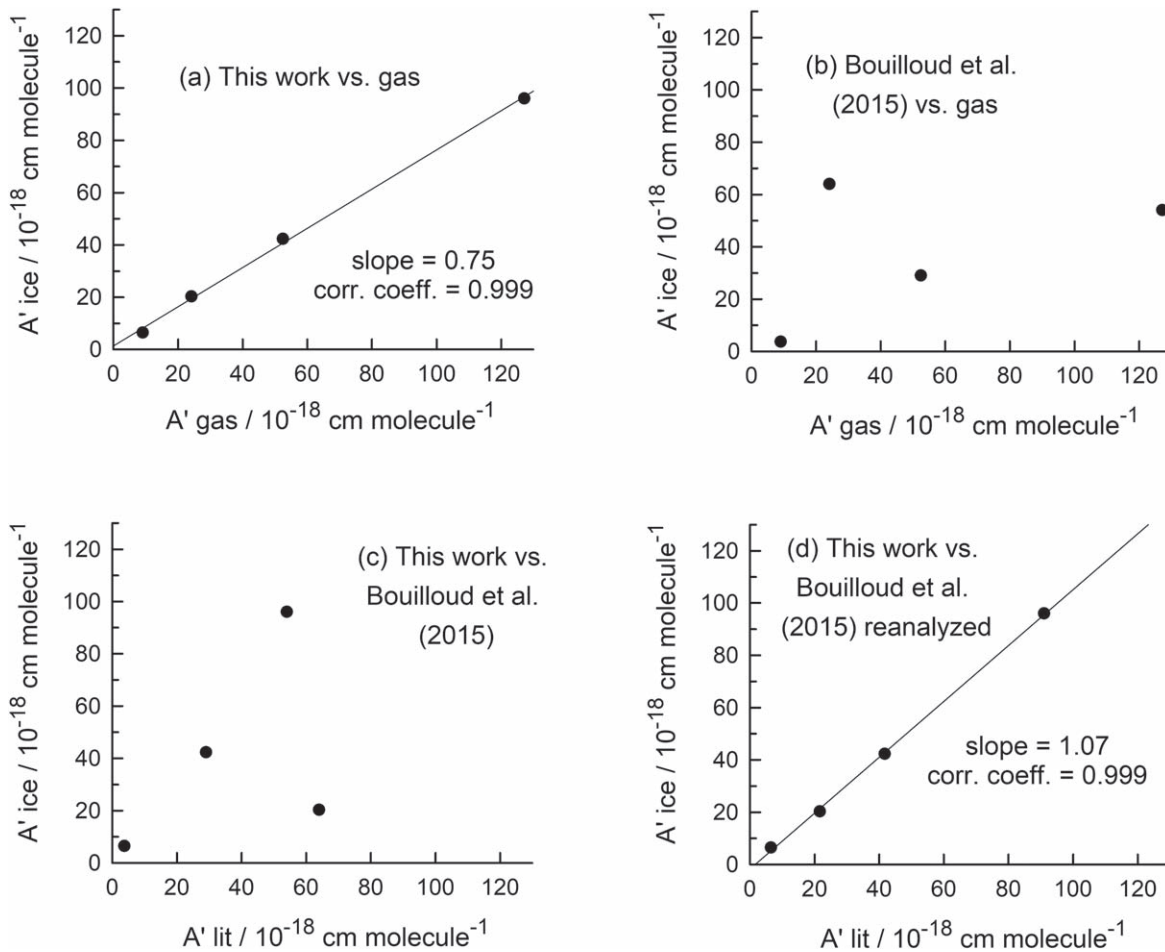
Figure 13. Comparisons of band strengths of amorphous (HCOOH)$_2$: (a) our work compared to gas-phase results of Y. Maréchal (1987); (b) band strengths of M. Bouilloud et al. (2015) compared to gas-phase results of Y. Maréchal (1987); (c) our work compared to results of M. Bouilloud et al. (2015); (d) our work compared to results from the spectrum of M. Bouilloud et al. (2015) after reintegration. See the text for details.

Table 13
Infrared Band Strengths of Selected Amorphous Ices[a]

Class	Compound	Position/cm^{-1}	$A'/(10^{-18}$ cm molec^{-1})	Reference
aldehyde	H$_2$CO formaldehyde	1724	16.3	This work
ketone	CH$_3$C(O)CH$_3$ acetone	1711	26.7	R. L. Hudson et al. (2018)
ester	HC(O)OCH$_3$ methyl formate	1721	48.3	Y. Y. Yarnall & R. L. Hudson (2022c)
acid	(HCOOH)$_2$ formic acid	1712	96.0	This work

Note.
[a] All ices and measurements were made near 10 K. Some compounds have more than one name.

$(96.1 \times 10^{-18}) / 2 = 48.0 \times 10^{-18}$ cm molecule^{-1}, which is comparable to that listed for methyl formate. The measured ratio of C=O dimer-to-monomer IR intensities of gas-phase formic acid is about 1.4 (Y. Maréchal 1987), so an argument might be made that division by 1.4 is a better approach.

We note in passing that our IR spectrum of amorphous formic acid has a small feature at 1074 cm^{-1} near where the intense C–O vibrational mode of monomeric HCOOH is expected (Y. Maréchal 1987). Our ice was made by condensation of formic acid vapor with a pressure near 30 Torr at ∼20°C. Under these conditions, the vapor will be overwhelmingly composed of the dimer, which then is condensed to make an ice. See A. S. Coolidge (1929) for more on the monomer-dimer equilibrium. Further work at higher vapor temperatures and lower vapor pressures will shift the gas-phase equilibrium toward the monomer in the gas phase before condensation. For now, we assign the 1074 cm^{-1} feature in our spectra to (HCOOH)$_2$.

8.6. Vapor Pressures and Sublimation Enthalpies

Little can be said about comparisons of our sublimation pressures for solid HNCO and solid H$_2$CO to literature results as no others have been found. Our sublimation enthalpies are 43.1 kJ mol^{-1} for HNCO and $\Delta H_{subl} = 34.8$ kJ mol^{-1} for H$_2$CO. As expected, each of these is larger than the enthalpy of vaporization of the corresponding liquid, $\Delta H_{vap}(\text{HNCO}) = 30.7$ kJ mol^{-1} (W. Acree & J. S. Chickos 2010) and $\Delta H_{vap}(\text{H}_2\text{CO}) = 23.3$ kJ mol^{-1} (R. Spence & W. Wild 1935).

Vapor pressures and sublimation enthalpies can be useful in the study of stabilities of ices in the solar system as well as

those in the interstellar medium. A recent study of ices on Pluto and Kuiper Belt object Arrokoth (C. M. Lisse et al. 2021) specifically noted the paucity of thermodynamic data for solid H_2CO. Lacking such, the authors adopted "with caution" a value of $\Delta H_{subl} = 34 \, kJ \, mol^{-1}$ for solid formaldehyde, a serendipitous choice in close agreement with our value of $34.8 \, kJ \, mol^{-1}$.

8.7. IR Spectral Intensities of $H_2O + H_2CO$ Ices

Figure 8 shows that good linearity was found for formaldehyde absorbances as a function of H_2CO column density in our $H_2O + H_2CO$ ices. Table 9 shows that the formaldehyde band strengths in the H_2O-rich ices were about 4% to 10% less than those of neat amorphous H_2CO. This small influence of H_2O ice on band strengths matches what we found earlier for solid HCN, H_2S, SO_2, and OCS (P. A. Gerakines et al. 2022; Yarnall & Hudson 2022b), but it contrasts with a greater influence in the case of band strengths of CH_3OH ices (R. L. Hudson et al. 2024). We suspect that the influence of H_2O ice depends on the extent of hydrogen bonding of the "guest" compound (i.e., CH_3OH, etc). Few cases have been examined quantitatively so far, hindering a firm conclusion.

8.8. Recommendations and Needs

Our intensity results should find wide use among laboratory astrochemists with interests in icy solids. For example, we have shown that band strengths of H_2CO can be used to make H_2O-rich mixtures of accurately known composition that then can be characterized spectroscopically (e.g., band strengths, peak positions, and peak widths). The same is possible for HNCO in ices dominated by H_2O or other species.

Some previous investigations that aimed for quantitative results might need reconsideration in light of the IR band strengths we are reporting. This is particularly true for laboratory measurements of reaction yields, such as in photo- and radiation chemical processes. The optical constants we report were measured by transmission through a CsI substrate, but they can be used to model spectra recorded by reflection from a metal surface (e.g., S. G. Tomlin 1968).

Observational infrared astronomers now have a firmer set of IR results in the search for and the quantification of interstellar and planetary ice components. In general, we do not recommend the older results, because they cannot be independently reproduced and because of the large number of uncertainties involved.

An observational problem in which we have long had an interest (R. L. Hudson et al. 2001) is the interstellar IR band for the cyanate anion (OCN^-), found near $2165 \, cm^{-1}$ ($4.62 \, \mu m$). As hard as it is to believe, there is still no firm IR band strength for this feature. Those commonly used can be traced to the paper of F. A. van Broekhuizen et al. (2004) about which we already have described multiple problems and concerns. New quantitative measurements involving HNCO should now be possible, free of earlier assumptions and uncertainties.

Perhaps the least satisfying part of our study concerns formic acid because our band strengths are for the dimer and not the monomer. It is somewhat hard to believe that $(HCOOH)_2$ will form in interstellar ices instead of HCOOH, so what still is needed are band strengths for the latter in H_2O-rich ices, but we know of no such results available. This gap in the literature can serve as a challenge for the experimentalist, an opportunity for the theorist, and a caution for infrared observers.

We end by noting that it is both surprising and disturbing that sometimes questionable and sometimes erroneous IR results for HNCO, H_2CO, and HCOOH ices have been carried forward in the literature for decades with little critical examination.

9. Summary and Conclusions

Infrared intensities have been quantified for the first time using established laboratory methods, and free of assumptions, for HNCO, H_2CO, and HCOOH, with each compound known to be extraterrestrial in the gas phase and suspected to be present in the solid phase. Solid-phase intensity results for each have been compared to those in the literature. For each compound, problems with the earlier studies exist so that IR band strengths already reported for these compounds are not recommended for laboratory or observational work. We also have measured the first vapor pressures for HNCO and H_2CO solids, along with enthalpies of sublimation. Densities and refractive indices for HNCO, H_2CO, and HCOOH are presented. A caution and challenge are offered regarding formic acid.

ORCID iDs

Reggie L. Hudson ⓘ https://orcid.org/0000-0003-0519-9429
Yukiko Y. Yarnall ⓘ https://orcid.org/0000-0003-0277-9137
Perry A. Gerakines ⓘ https://orcid.org/0000-0002-9667-5904

References

Acree, W., Jr., & Chickos, J. S. 2010, JPCRD, 39, 043101
Altwegg, K., Balsiger, H., Hanni, N., et al. 2020, NatAs, 4, 533
Bouilloud, M., Fray, N., Bénilan, Y., et al. 2015, MNRAS, 451, 2145
Brown, S. S., Berghout, H. L., & Crim, F. F. 1997, JChPh, 107, 9764
Coffey, M. J., Berghout, H. L., Woods, E., III, & Crim, F. F. 1999, JChPh, 110, 10850
Congiu, E., Sow, A., Nguyen, T., Baouche, S., & Dulieu, F. 2020, RScI, 91, 124504
Coolidge, A. S. 1929, JAChS, 50, 2166
Cottin, H., Moore, M. H., & Benilan, Y. 2003, ApJ, 590, 874
Cyriac, J., & Pradeep, T. 2005, CPL, 402, 116
de Barros, A. L.-F., Mejía, C., Seperuelo Duarte, E., et al. 2022, MNRAS, 511, 2491
Denbigh, K. G. 1940, Trans. Faraday Soc., 36, 936
d'Hendecourt, L. B., & Allamandola, L. J. 1986, A&AS, 64, 453
Evers, J., Krumm, B., Axthammer, Q. J., et al. 2018, JPCA, 122, 3287
Fray, N., & Schmitt, B. 2009, P&SS, 57, 2053
Gerakines, P. A., & Hudson, R. L. 2015a, ApJ, 805, L20
Gerakines, P. A., & Hudson, R. L. 2015b, ApJ, 808, L40
Gerakines, P. A., & Hudson, R. L. 2020, ApJ, 901, 1
Gerakines, P. A., Materese, C. K., & Hudson, R. L. 2023, MNRAS, 526, 4051
Gerakines, P. A., Yarnall, Y. Y., & Hudson, R. L. 2022, MNRAS, 509, 3515
Gerakines, P. A., Yarnall, Y. Y., & Hudson, R. L. 2024, Icar, 413, 1
Halfen, D. T., IIyushin, V. V., & Ziurys, L. M. 2015, ApJL, 812, L5
Halupka, M., & Sander, W. 1998, AcSpA, 54A, 495
Harvey, K. B., & Ogilvie, J. F. 1962, CaJCh, 40, 85
Herczku, P., Mifsud, D. V., Ioppolo, S., et al. 2021, RScI, 92, 084501
Hollenberg, J. L., & Dows, D. A. 1961, JChPh, 34, 1061
Hudson, R. L. 2016, PCCP, 18, 25756
Hudson, R. L., & Coleman, F. M. 2019, PCCP, 211, 11284

Hudson, R. L., Ferrante, R. F., & Moore, M. H. 2014a, Icar, 228, 276
Hudson, R. L., Gerakines, P. A., & Ferrante, R. F. 2018, AcSpA, 193, 33
Hudson, R. L., Gerakines, P. A., & Moore, M. H. 2014b, Icar, 243, 148
Hudson, R. L., Gerakines, P. A., & Yarnall, Y. Y. 2022a, ApJ, 925, 1
Hudson, R. L., Gerakines, P. A., & Yarnall, Y. Y. 2023, Icar, 396, 115499
Hudson, R. L., Gerakines, P. A., & Yarnall, Y. Y. 2024, ApJ, 970, 1
Hudson, R. L., Loeffler, M. J., Ferrante, R. F., Gerakines, P. A., &
    Coleman, F. M. 2020a, ApJ, 891, 22
Hudson, R. L., Loeffler, M. J., & Gerakines, P. A. 2017, JChPh, 146, 0243304
Hudson, R. L., & Moore, M. H. 1995, RaPC, 45, 779
Hudson, R. L., & Moore, M. H. 1999, Icar, 140, 451
Hudson, R. L., & Moore, M. H. 2000, Icar, 145, 661
Hudson, R. L., Moore, M. H., & Gerakines, P. A. 2001, ApJ, 550, 1140
Hudson, R. L., & Yarnall, Y. Y. 2022a, ESC, 6, 1163
Hudson, R. L., & Yarnall, Y. Y. 2022b, Icar, 377, 1
Hudson, R. L., Yarnall, Y. Y., & Coleman, F. C. 2020b, AcSpA, 233, 118217
Hudson, R. L., Yarnall, Y. Y., & Gerakines, P. A. 2022b, AsBio, 22, 452
Hudson, R. L., Yarnall, Y. Y., & Gerakines, P. A. 2022c, PSJ, 3, 1
Kekulé, A. 1892, Ber. Dtsch. Chem. Ges., 25, 2435
Khanna, R. K., Allen, J. E., Masterson, C. M., & Zhao, G. 1990, JPhCh, 94, 440
Khoshkhoo, H., & Nixon, E. R. 1973, AcSpA, 29, 603
Lis, D. C., Keene, J., Young, K., et al. 1997, Icar, 130, 355
Lisse, C. M., Young, L. A., Cruikshank, D. P., et al. 2021, Icar, 356, 114072
Lowenthal, M. S., Khanna, R. K., & Moore, M. H. 2002, AcSpA, 58, 73
Lu, C. S., & Lewis, O. 1972, JAP, 43, 4385
Maréchal, Y. 1987, JChPh, 87, 6344
Martín-Doménech, R., DelFranco, A., Öberg, K. I., & Rajappan, M. 2024, ApJ,
    962, 1
Materese, C. K., Gerakines, P. A., & Hudson, R. L. 2021, Acc. Chem. Res.,
    54, 280
McClure, M. K., Rocha, W. R.-M., Pontoppidan, K. M., et al. 2023, NatAs,
    7, 431
Millikan, R. C., & Pitzer, K. S. 1957, JChPh, 27, 1305
Millikan, R. C., & Pitzer, K. S. 1958, JAChS, 80, 3515
Moore, M. H., Ferrante, R. F., Moore, W. J., & Hudson, R. L. 2010, ApJS,
    191, 96
Potapov, A., Krasnokutski, S. A., Jäger, C., & Henning, T. 2021, ApJ, 920, 111

Raunier, S., Chiavassa, T., Marinelli, F., Allouche, A., & Aycard, J. P. 2003,
    CPL, 368, 594
Rocha, W. R.-M., Perotti, G., Kristensen, L. E., & Jørgensen, J. K. 2021, A&A,
    654, A158
Rodríguez-Almeida, L. F., Rivilla, V. M., Jiménez-Serra, I., et al. 2021, A&A,
    654, L1
Schneider, W. G., & Bernstein, H. J. 1956, Trans. Faraday Soc., 52, 13
Schutte, W. A., Allamandola, L. J., & Sandford, S. A. 1993, Icar, 104, 118
Schutte, W. A., Boogert, A. C.-A., Tielens, A. G.-G. M., et al. 1999, A&A,
    343, 966
Schutte, W. A., Gerakines, P. A., Geballe, T. R., van Dishoeck, E. F., &
    Greenberg, J. M. 1996, A&A, 309, 633
Snyder, L. E., & Buhl, D. 1972, ApJ, 177, 619
Snyder, L. E., Buhl, D., Zuckerman, B., & Palmer, P. 1969, PhRvL, 22, 679
Snyder, L. E., Palmer, P., & de Pater, I. 1989, AJ, 97, 243
Soifer, B. T., Puetter, R. C., Russell, R. W., et al. 1979, ApJL, 232, L53
Spence, R., & Wild, W. 1935, J. Chem. Soc., 1935, 506
Tempelmeyer, K. E., & Mills, D. W. 1968, JAP, 39, 2968
Thakur, T. S., Kirchner, M. T., Bläser, D., Boese, R., & Desiraju, G. R. 2011,
    PCCP, 13, 14076
Tomlin, S. G. 1968, JPhD, 2, 1667
Tsuge, M., Hidaka, H., Kouchi, A., & Watanabe, N. 2020, ApJ, 900, 1
Urso, R. G., Baklouti, D., Djouadi, Z., Pinilla-Alonso, N., & Brunetto, R. 2020,
    ApJL, 894, L3
van Broekhuizen, F. A., Keane, J. V., & Schutte, W. A. 2004, A&A, 415, 425
von Dohlen, W. C., & Carpenter, G. B. 1955, AcCry, 8, 646
Weast, R. C., & Astle, M. J. 1980, CRC Handbook of Data on Organic
    Compounds (Boca Raton, Florida: CRC Press)
Weast, R. C., & Astle, M. J. 1985, CRC Handbook of Data on Organic
    Compounds (Boca Raton, Florida: CRC Press)
Winnewisser, G., & Churchwell, E. 1975, ApJL, 200, 33
Yamada, H., & Person, W. B. 1964, JChPh, 41, 2478
Yang, Y.-L., Green, J. D., Pontoppidan, K., et al. 2022, ApJ, 941, L13
Yarnall, Y. Y., & Hudson, R. L. 2022a, Icar, 373, 114799
Yarnall, Y. Y., & Hudson, R. L. 2022b, ApJL, 91, L4
Yarnall, Y. Y., & Hudson, R. L. 2022c, AcSpA, 283, 121738
Zuckerman, B., Ball, J. A., & Gottlieb, C. A. 1971, ApJL, 163, 41